Neuron, Vol. 14, 43–56, January, 1995, Copyright © 1995 by Cell Press

Targeted Disruption of Ca^{2+}-calmodulin Signaling in Drosophila Growth Cones Leads to Stalls in Axon Extension and Errors in Axon Guidance

Mark F. A. VanBerkum and Corey S. Goodman
Howard Hughes Medical Institute
Division of Neurobiology
Department of Molecular and Cell Biology
Life Science Addition Room 519
University of California, Berkeley
Berkeley, California 94720

Summary

Ca^{2+}-calmodulin (CaM) function was selectively disrupted in a specific subset of growth cones in transgenic Drosophila embryos in which a specific enhancer element drives the expression of the kinesin motor domain fused to a CaM antagonist peptide (kinesin-antagonist or KA, which blocks CaM binding to target proteins) or CaM itself (kinesin-CaM or KC, which acts as a Ca^{2+}-binding protein). In both KA and KC mutant embryos, specific growth cones exhibit dosage-dependent stalls in axon extension and errors in axon guidance, including both defects in fasciculation and abnormal crossings of the midline. These results demonstrate an in vivo function for Ca^{2+}-CaM signaling in growth cone extension and guidance and suggest that Ca^{2+}-CaM may in part regulate specific growth cone decisions, including when to defasciculate and whether or not to cross the midline.

Introduction

During development, neuronal growth cones traverse a variety of terrains containing an array of both attractive and repulsive guidance molecules, including extracellular matrix components, cell adhesion molecules, and other cell surface ligands on neighboring cells and neurites, and chemoattractive or chemorepulsive cues secreted from more distal cells (reviewed by Goodman and Shatz, 1993; Goodman, 1994). Individual growth cones are presumably covered with a variety of different receptors that help them discriminate between these extracellular signals and transduce them into meaningful cytoplasmic signals that regulate growth cone motility, extension, and guidance, and ultimately, the transformation of the growth cone into a presynaptic terminal.

Extensive in vitro assays have begun to reveal certain components of growth cone signal transduction machinery (e.g., Schuch et al., 1989; Doherty and Walsh, 1994). Nevertheless, little is known about what aspects of growth cone behavior in vivo are controlled by these signaling pathways. Moreover, given the recent discoveries of new families of guidance signals (e.g., Kolodkin et al., 1992, 1993; Luo et al., 1993; Serafini et al., 1994; Kennedy et al., 1994), we are still a long way from having a coherent picture of the range of downstream signaling systems within the growth cone and how they interact to govern growth cone behavior.

Ca^{2+} has been implicated in the regulation of a wide range of growth cone behaviors (Kater and Mills, 1991; Cypher and Letourneau, 1992). For example, increases in internal Ca^{2+} have been associated with axonogenesis (Silver et al., 1990; Bentley et al., 1991), axon turning (Zheng et al., 1994), specific growth cone contacts (Bentley et al., 1991), changes in filopodial morphology (Davenport and Kater, 1992; Rehder and Kater, 1992), certain kinds of growth cone collapse in vitro (Bandtlow et al., 1993), and cell adhesion molecule–mediated neurite outgrowth in vitro (e.g., Doherty and Walsh, 1994). Although a few actin- or microtubule-binding proteins may interact directly with Ca^{2+} (Janmey, 1994; Lee, 1993), much of the Ca^{2+} signal is undoubtedly transduced by calmodulin (CaM), a major intracellular receptor for Ca^{2+} (e.g., Gnegy, 1993; Hinrichsen, 1993). CaM, with over 20 target proteins known to be involved in cyclic nucleotide metabolism, energy metabolism, secretion, and cytoskeletal dynamics, is well suited to be an important mediator of Ca^{2+} signaling and regulator of growth cone behavior. Indeed, pharmacological inhibitors of CaM can, for example, prevent the decrease in neurite outgrowth in response to increases in intracellular Ca^{2+} (Polak et al., 1991). Overexpression of CaM-dependent protein kinase II (CaMKII), a major substrate for CaM (Hanson and Schulman, 1992), in cultured neuroblastoma cells results in increased neurite outgrowth (Goshima et al., 1993). Thus, there is much circumstantial evidence that Ca^{2+} and its major intracellular receptor, CaM, play important roles in growth cone signal transduction. However, in some respects, Ca^{2+} signaling has been implicated in so many aspects of growth cone behavior that it is difficult to predict which of these behaviors it really controls in vivo and which receptor systems transduce their signals via this pathway.

One way to begin to elucidate the in vivo function(s) of Ca^{2+} signaling in growth cone behavior would be to perturb specifically this signal transduction pathway in particular growth cones in the developing embryo. Our goal in the present study has been to use the power of genetics in Drosophila melanogaster to target specifically the disruption of Ca^{2+}–CaM function in particular growth cones in the developing embryo. To this end, we used transposon-mediated transformation methods to generate transgenic fruitflies carrying transposons with control elements that drive the expression of specific fusion proteins in a defined subset of identified neurons; these fusion proteins are constructed such that they will be targeted for the growth cone and will either block CaM binding to target proteins or CaM binding to Ca^{2+}.

The plethora of CaM-regulated events makes it difficult to use null mutations in the *calmodulin* gene to address the specific role of CaM in growth cone guidance (Doyle et al., 1990; K. Beckingham, personal communication). Moreover, the loading of the embryo with maternally derived CaM makes it difficult to conduct traditional loss-of-function genetic analysis of these events (Kovalick and Beckingham, 1992). We circumvented these problems by

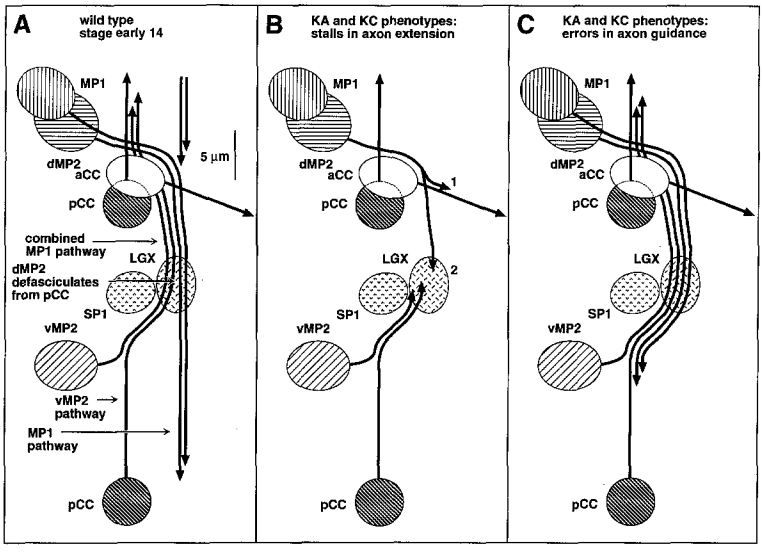

Figure 1. Development of the vMP2 and MP1 Pathways in Wild-Type versus KA and KC Stage 14 Mutant Embryos

(A) Diagrams based on light and electron microscopy of stage early 14 wild-type embryos (Lin et al., 1994; R. Fetter et al., unpublished data). The circles show the size and location of the nuclei of identified neurons (MP1, dMP2, vMP2, SP1, pCC, and aCC) and glia (LGX). The lines and arrows show the locations of the axons and growth cones of these neurons at this stage. The vMP2 pathway is pioneered by pCC with vMP2 following close behind. The MP1 pathway is pioneered by dMP2, with MP1 following close behind. For part of the distance within each segment, pCC and dMP2 fasciculate to form the combined MP1 pathway. Around the middle of LGX, dMP2 defasciculates from pCC and forms the independent MP1 pathway.

(B and C) When Ca^{2+}-CaM signaling is disrupted in the MP1 pathway growth cones in KA and KC mutant embryos, we observe two classes of phenotypes at stage 14: stalls in axon extension at specific choice point locations (B) and errors in axon guidance at specific choice point locations (C).

(B) In some segments, dMP2 stalls around the aCC initial axon segment (1), where normally it would display only a transient affinity before turning posteriorly. In other segments, dMP2 extends posteriorly and then stalls around the LGX glial cell (2), where normally it would defasciculate from pCC and continue extending posteriorly to pioneer its own pathway.

(C) In some segments, dMP2 continues to extend but fails to defasciculate properly from pCC at the LGX glial cell location, and instead, dMP2 and MP1 extend more medially as they remain fasciculated in the vMP2 pathway.

designing two dominant inhibitors of CaM function and then expressing them using a specific enhancer element that drives expression in a set of well-characterized neurons (e.g., pCC, vMP2, dMP2, and MP1) whose axons pioneer two well-described axon pathways: the MP1 and vMP2 pathways (Hiromi et al., 1985; Doe et al., 1988). In addition, we targeted these CaM function inhibitors to the growth cone by using the motor domain of kinesin, a microtubule-dependent ATPase involved in fast axonal transport (Skoufias and Scholey, 1993). kinesin has been used previously to target β-galactosidase (β-gal) fusion proteins to the growth cone (Giniger et al., 1993).

The interaction between CaM and some of its target enzymes, in particular smooth and skeletal muscle myosin light chain kinases (MLCKs), has been characterized in great detail (e.g., reviews by Means et al., 1991; Weinstein and Mehler, 1994). When CaM binds Ca^{2+}, it interacts with the basic amphipathic helix of the CaM-binding domain of a target enzyme and removes an overlapping autoinhibitory domain from the catalytic site. The interactions between CaM and synthetic peptide analogs of this regulatory domain have been studied extensively using enzymatic (e.g., Bagchi et al., 1992; Bowman et al., 1992; Gao et al., 1993; Persechini et al., 1994) and biophysical (e.g., Chattopadhyaya et al., 1992; Ikura et al., 1992; Knighton et al., 1992; Trewhela, 1992; Gough and Taylor, 1993) techniques; a crystal structure of this interaction is now available (Meador et al., 1992, 1993). Synthetic peptide analogs of this binding region are highly specific competitive inhibitors of CaM (IC_{50} of about 1 nM) both in vitro (VanBerkum and Means, 1991) and in vivo (McCarron et al., 1992).

We attached the CaM-binding domain of MLCK to the C-terminus of the motor domain of kinesin to create a fusion protein we term kinesin–antagonist (KA). KA should be targeted to the growth cone by kinesin-mediated microtubule transport and then function as a potent inhibitor of CaM in the growth cone. In principle, as the intracellular Ca^{2+} levels rise in the growth cone (possibly in response to guidance cues), endogenous CaM will bind to Ca^{2+}, KA will act as a functionless but potent CaM-binding protein, and thus much of the normal CaM-mediated signaling will be prevented. Similarly, a potent Ca^{2+}-binding protein was targeted to the growth cone by attaching chicken CaM to the C-terminus of the kinesin motor domain (kinesin–CaM [KC]). This protein competes with endogenous CaM or other Ca^{2+}-binding proteins for available Ca^{2+}. From available structure–function studies on CaM and CaM activation of target enzymes, owing to the location and size of the kinesin attachment, KC is predicted to be unable to activate CaM-dependent enzymes (Zot et al., 1990; VanBerkum and Means, 1991; Persechini et al., 1994).

To drive the expression of these fusion proteins, we used the *fushi tarazu* (*ftz*) neurogenic (ftz_{ng}) control element (Hiromi et al., 1985) because it has previously been shown to drive the expression of β-gal (Doe et al., 1988) in a specific subset of identified neurons, including the pCC, vMP2, dMP2, and MP1 neurons, whose growth cones pioneer the first two longitudinal axon pathways (the vMP2 and MP1 pathways) and whose axon pathfinding has been studied in great detail (Lin et al., 1994). We assessed the role of Ca^{2+}–CaM signaling in these growth cones by monitoring their behavior and the formation of the MP1 and vMP2 pathways in KA or KC transformants. Expression of both KA and KC fusion proteins in stable transformants leads to dosage-dependent stalls in neurite extension, defects in fasciculation, and abnormal crossings of the midline. Transformants expressing just the kinesin motor do-

main or a kinesin–β-gal chimeric were indistinguishable from wild-type embryos. This study provides in vivo evidence that Ca^{2+} signaling in the growth cone is required for proper axon pathfinding. Moreover, these results suggest that Ca^{2+} may in part regulate certain growth cone decisions, including whether or not to cross the midline.

Results

Development of the vMP2 and MP1 Pathways

The first two longitudinal axon pathways to form in the CNS of the Drosophila embryo are the vMP2 and MP1 fascicles (Figure 1A). The formation of these pathways during stages 13–14 has been studied extensively using two different monoclonal antibodies (the 22C10 and 1D4 anti-fasciclin II MAbs) in light microscopy and extensive electron microscopic serial section reconstructions (Lin et al., 1994; R. D. Fetter, C. Kopczynski, V. Auld, G. Grenningloh, and C. S. G., unpublished data); the same two MAbs are used here to follow the development of these two pathways in transgenic embryos in which Ca^{2+}–CaM function is disrupted in specific vMP2 and MP1 pathway growth cones.

In wild-type embryos at stage late 12, the pCC growth cone begins to extend anteriorly to pioneer the vMP2 pathway. The vMP2 growth cone then follows behind pCC and tightly fasciculates with pCC. The pCC growth cone continues to extend anteriorly as it jogs laterally and internally toward the cell body of the SP1 neuron and a specific glial cell called LGX. pCC's growth cone extends along the medial surface of LGX. pCC and vMP2 adhere to each other and to LGX, with vMP2 being more medial and also adhering to the SP1 cell body. About this time, the dMP2 growth cone extends laterally along the aCC axon and then turns posteriorly. The MP1 growth cone tightly fasciculates with dMP2 and extends behind it. When the posteriorly extending dMP2 growth cone meets the anteriorly extending pCC growth cone at stage late 13, they tightly fasciculate together, forming the combined MP1 pathway. Once the dMP2 growth cone has reached the next posterior segment, at a specific location (Figure 1A) it abruptly defasciculates from pCC at stage mid 13. Rather than extending along the more medial vMP2 pathway, it instead extends posteriorly in a more lateral location to pioneer the MP1 pathway, which is complete by stage early 14. In this way, two pathways form within each segment: the vMP2 and the MP1 fascicles. Between the segments, these two pathways are fused in the combined MP1 pathway (Figure 1A).

Using the ftz_{ng} Element and the kinesin Motor Domain to Drive Fusion Proteins into the Growth Cones of Specific Neurons

We used the ftz_{ng} control element (Hiromi et al., 1985), a well-characterized 1.4 kb piece of genomic DNA from the 5′ flanking region of the *ftz* gene, to drive the expression of CaM inhibitors in a subset of CNS neurons, including those (pCC, vMP2, dMP2, and MP1) whose axons pioneer the vMP2 and MP1 pathways. Based on the expression pattern of the ftz_{ng} element (Doe et al., 1988), we suspected

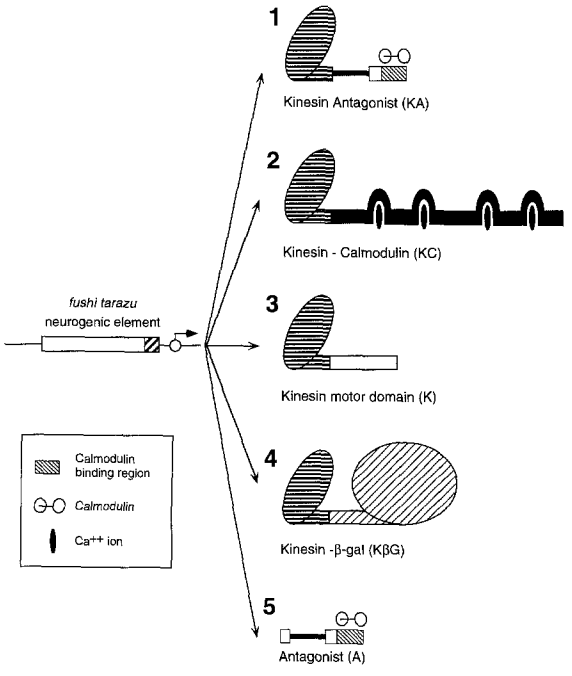

Figure 2. Minigene Constructs Encoding Fusion Proteins Used to Examine Ca^{2+}-CaM Signaling in the Growth Cone

We used the ftz_{ng} control element to drive the expression of five different minigenes in the neurons whose axons pioneer the vMP2 and MP1 pathways (pCC, vMP2, dMP2, and MP1). Ca^{2+}-CaM signaling in the growth cone was selectively inhibited using the kinesin motor domain to drive a CaM antagonist peptide (1) or CaM itself (2) into the growth cone. A kinesin–antagonist (KA) protein was created by removing the CaM regulatory domain (plus flanking sequences) from MLCK and attaching it to the C-terminus of the kinesin motor domain (1). KA will compete with other CaM target proteins for Ca^{2+}-CaM and thus prevent much of the CaM-mediated signaling in the growth cones of these neurons. A second kinesin fusion protein was created by attaching a wild-type chicken CaM to the C-terminus of the motor domain of kinesin to create kinesin–CaM (KC), a Ca^{2+}-binding protein (2). KC should inhibit CaM (and other Ca^{2+}-binding proteins) by competing for available Ca^{2+}. The third minigene (3) encodes just the kinesin motor domain (K); the fourth minigene (4) encodes kinesin attached to β-gal (KβG). These two proteins (3 and 4) serve as controls to ensure that the kinesin portion of KA or KC is not responsible for the altered growth cone behavior. Finally, to test whether the CaM binding antagonist peptide needs to be translocated to the growth cone in order to exert its effect on growth cone behavior, the fifth minigene (5) encodes just the CaM-binding domain of MLCK (A; the same portion as used in KA). Without the kinesin motor domain, this CaM-binding peptide is expected to be distributed diffusely in the cell body and processes.

that this regulatory element might allow us to manipulate Ca^{2+} signaling in these same growth cones and thus analyze the resulting defects in axon pathfinding. Recent studies have shown that ftz_{ng} transgenes drive fasciclin II expression on the growth cones and axons of pCC, vMP2, dMP2, and MP1 at stages 13–14 (Lin et al., 1994). The ftz_{ng} element also drives expression of fasciclin II on the axons in the FN3 pathway, which can be visualized at stage 16 using the 1D4 MAb.

Thus, we used the ftz_{ng} element to drive the expression of five different minigenes (Figure 2) in the neurons whose axons pioneer the vMP2 and MP1 pathways (pCC, vMP2,

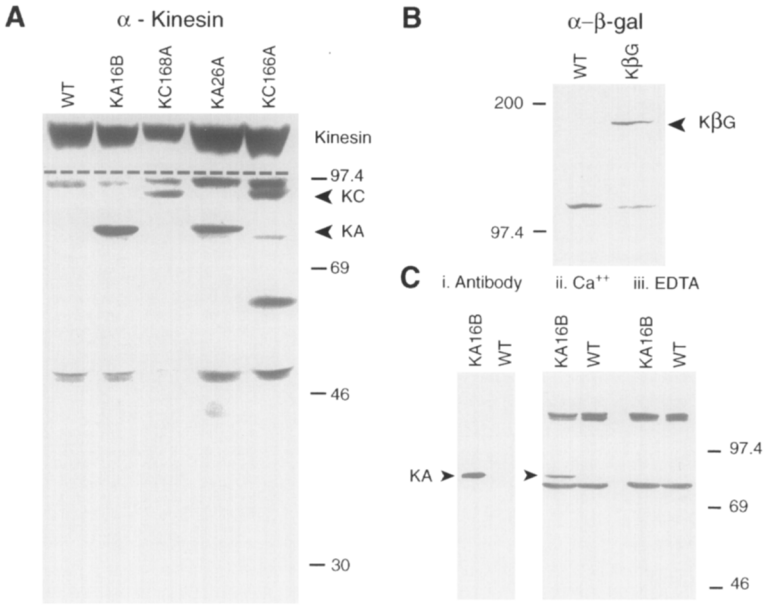

Figure 3. Biochemical Characterization of Fusion Proteins

(A) kinesin fusion proteins were co-pelleted with microtubules and identified by Western blot techniques using an anti-kinesin antibody. Native kinesin (115 kDa) is present in all lanes. The KA and KC fusion proteins (arrowheads) are present only in the KA and KC transgenic lines, respectively. The protein present in all lanes at variable amounts at ~97 kDa probably represents a degradation product of native kinesin. The protein at ~62 kDa is consistently present only in extracts from the KC166A line. The protein at ~49 kDa is background staining of tubulin. The blot was cut at the dotted line, and each portion was probed separately and developed for 10 s (top) or 10 min (bottom). WT, wild type; KA16B, KA26A, KC168A, and KC166A: different KA and KC transgenic lines, respectively.

(B) Same as in (A), but using an antibody against β-gal. Lower band is native kinesin detected by anti-kinesin that had not been completely stripped off of the blot. KβG, kinesin–β-gal.

(C) In the left pair of KA16B versus WT blots (i), KA (arrowhead) is the sole protein recognized by an antibody raised against the CaM-binding domain of KA. In the middle and right pair of blots (ii and iii), only the KA protein (arrowhead) binds CaM in a Ca^{2+}-dependent manner, as detected in this CaM overlay assay. The other bands represent nonspecific electrostatic interactions with either CaM or the HRP-conjugated Streptavidin used in this assay. Positions of the molecular mass standard in kilodaltons are indicated in all panels.

dMP2, and MP1). We monitored the consequence of expressing these fusion proteins on growth cone guidance using the 22C10 and 1D4 MAbs. It is experimentally possible to target these proteins into the growth cone selectively using the kinesin motor domain (Giniger et al., 1993). When the *ftz*$_{ng}$ element was used to drive the expression of the axon marker kinesin–β-gal (KβG; Giniger et al., 1993), consisting of the motor domain of kinesin fused to the *lacZ* gene, β-gal activity at stage 13 was observed primarily in the growth cones of the dMP2 and vMP2 neurons (D. Van Vactor, personal communication).

In the first two minigenes, Ca^{2+}–CaM signaling in the growth cone was selectively inhibited by using the kinesin motor domain to drive a CaM antagonist peptide or CaM itself into the growth cone. A KA protein was created by removing the CaM regulatory domain (plus flanking sequences) from the chicken MLCK (see Introduction for rationale) and attaching it to the C-terminus of the kinesin motor domain (Figure 2). KA will compete with other CaM target proteins for Ca^{2+}–CaM, and thus prevent much of the CaM-mediated signaling in the growth cones of these neurons. A second kinesin fusion protein was created by attaching a wild-type chicken CaM to the C-terminus of the motor domain of kinesin to create KC, a Ca^{2+}-binding protein. KC should inhibit CaM (and other Ca^{2+}-binding proteins) by competing for available Ca^{2+}. It is predicted from structure–function studies that KC should not activate CaM target proteins directly (see Introduction).

The third minigene encodes just the kinesin motor domain (K); the fourth minigene (D. Van Vactor, unpublished data) encodes kinesin attached to β-gal (KβG). These two proteins serve as controls to ensure that the kinesin portion of KA or KC is not responsible for the altered growth cone behavior. In addition, since K has an extra 35 amino acids attached to kinesin, it serves as a random peptide control for CaM antagonist activity. Finally, to test whether the CaM-binding antagonist peptide needs to be translocated to the growth cone in order to exert its effect on growth cone behavior, a fifth minigene gene (A) was constructed that encodes just the CaM-binding domain of MLCK (the same portion used in KA). Without the kinesin motor domain, this CaM-binding peptide is expected to be distributed diffusely in the cell body and processes (and thus reduce the concentration in the growth cone by at least 10-fold). In all, 11 KA, 8 KC, 7 K, and 9 A independent transformant lines were isolated and maintained as balanced stocks; 1 previously made KβG line was also used.

Biochemical Characterization of Fusion Proteins

It was important to test to what extent the individual domains retained their biochemical properties in the context of these fusion proteins. First, we tested whether the KA, KC, and KβG fusion proteins would still bind microtubules (as does Kinesin on its own) by determining whether they were co-pelleted with microtubules in embryo extracts (Saxton et al., 1988). Indeed, Western blots revealed that Kinesin as well as the KA, KC, and KβG fusion proteins were enriched by these procedures (Figures 3A and 3B). KA and KC can also be released from microtubules with excess ATP (data not shown). Thus, the microtubule-binding and ATPase-dependent activity of the kinesin motor domain appears to be functional in these fusion proteins.

Second, we used a CaM overlay assay to show that chicken CaM binds to KA in a Ca^{2+}-dependent fashion in extracts enriched for KA by co-sedimentation with polymerized microtubules (Figure 3C). That this protein is KA is demonstrated by its ability to bind to the rat antibody

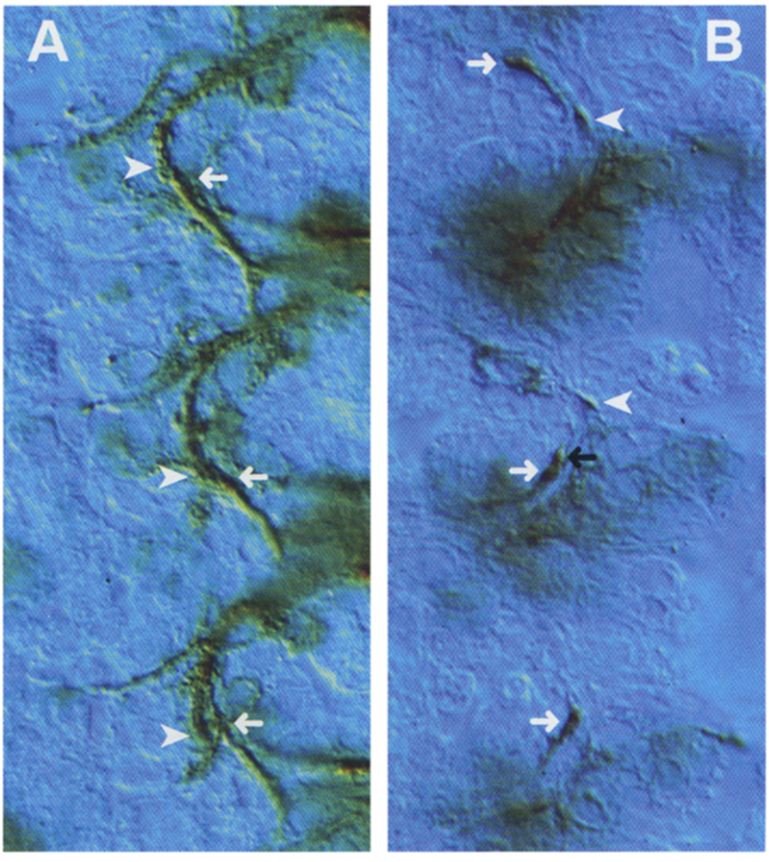

Figure 4. Expression of KA Fusion Protein in MP1 Pathway Growth Cones

Photographs of stage late 13 wild-type (A) or KA16B (B) embryos stained with either MAb 22C10 (A), which most darkly stains the dMP2 (white arrowhead) and vMP2 (white arrow) growth cones and axons, or MAb 10F4 (B), which recognizes the CaM-binding region of KA. At this stage (B), the KA fusion protein is clearly detected in the growth cones of dMP2 (white arrowhead), vMP2 (white arrow), and pCC (black arrow); the growth cones are stained much more darkly than are the axons, confirming that the kinesin motor domain has driven the fusion protein down into the growth cones. Different focal planes were combined digitally in this panel.

raised against the CaM-binding peptide (Figure 3C) and anti-kinesin antibodies (Figure 3A). Drosophila CaM, which differs from chicken CaM by only 3 out of 148 amino acids, activates chicken smooth muscle MLCK (from which the CaM-binding domain of KA was obtained) with kinetics identical to those of chicken CaM (Gao et al., 1993), and thus should also bind KA.

From the data on Ca^{2+} binding to CaM, including the conformational changes upon Ca^{2+} binding and the cooperativity of Ca^{2+} binding, it is anticipated that KC should retain the Ca^{2+}-binding properties of CaM. Indeed, like native CaM, a bacterially expressed version of KC binds to phenyl-Sepharose in a Ca^{2+}-dependent fashion (data not shown). KC should thus bind up to four Ca^{2+} ions at approximately 1 μM affinity (e.g., Beckingham, 1991).

The Expression of KA In Vivo

The biochemistry data suggest that these kinesin fusion proteins should be localized to the growth cone of the ftz_{ng}-expressing neurons by the translocation activity of kinesin. To confirm this putative growth cone localization, we used MAb 10F4, raised against the antagonist peptide (Figure 3C), to examine the localization of KA (Figure 4B). The 10F4 MAb recognized a peptide expressed in the appropriate ftz_{ng} pattern in KA transformant embryos but not wild-type controls. The ftz_{ng} enhancer element drives the expression of KA beginning at the end of stage 11 and continuing throughout embryogenesis, albeit at lower levels later in development. KA is present in the previously characterized segmentally repeating band of ftz_{ng}-expressing neurons (Doe et al., 1988; Lin et al., 1994). These neurons include aCC, pCC, vMP2, dMP2, and MP1 neurons, as well as some of the RP motoneurons, a number of other motoneurons, and other unidentified interneurons, some of whose axons fasciculate in the FN3 pathway.

Most important for this study, KA is present in the growth cones of the pCC, vMP2, dMP2, and MP1 neurons, the pioneers of the vMP2 and MP1 pathways, during stages 12–14 (Figure 4B). In general, vMP2 and pCC exhibit the highest levels of expression at stage 13 as compared with dMP2, MP1, and aCC; however, considerable variability in the relative levels of expression is observed both within and between different embryos. In KβG transformants, β-gal activity was also concentrated in the growth cones of these same neurons; the relative levels of KβG appear higher in dMP2 and vMP2 growth cones as compared with pCC and vMP2 growth cones at stage 13 (data not shown).

As development proceeds, the ftz_{ng} element remains active, although at reduced levels; however, KA expression is still observed in the same segmentally repeated pattern of neurons. In a previous study (Lin et al., 1994), the axon projections of many of these neurons were followed using the same ftz_{ng} element to drive the expression of an axon marker, tau–β-gal (Callahan and Thomas, 1994). By stage 16, most of the ftz_{ng}-expressing neurons extend their axons in the vMP2, MP1, or FN3 pathways. This is consistent

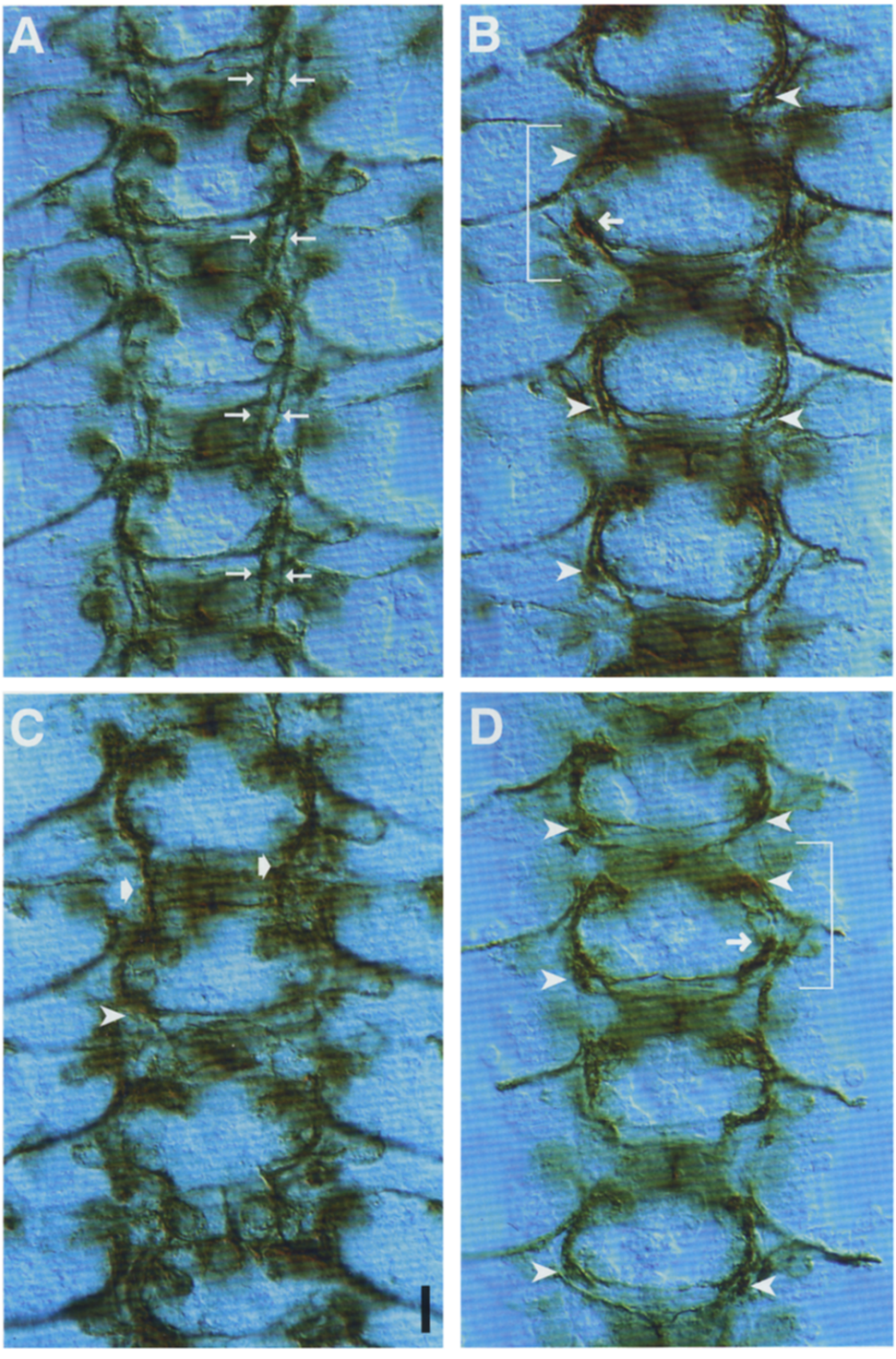

Figure 5. Stalls in Axon Extension and Errors in Growth Cone Guidance in KA and KC Mutant Embryos

Photographs of stage early 14 wild-type (A), KA (B and C), and KC (D) embryos stained with MAb 22C10, which reveals the axons and growth cones in the vMP2 and MP1 pathways. In wild-type embryos (A), the combined MP1 pathway between segments separates into two separate pathways within each segment: the more medial vMP2 pathway (white arrows pointing from left) and the more lateral MP1 pathway (white arrows pointing from right). Embryos homozygous for the KA (B and C) or KC (D) inserts display two classes of mutant phenotypes: stalls in axon extension and errors in axon guidance. Stalls in dMP2 extension are marked by the white arrowheads (B–D); stalls in vMP2 extension are marked by the white arrows (B and D). The absence of the MP1 pathway is marked by the white brackets in (B) and (D). In some segments, the dMP2 growth cone fails to defasciculate from pCC and instead continues to extend medially and posteriorly along the vMP2 pathway (short white arrows in [C]). See text for further details. Bar, 10 μm.

Table 1. Absence of MP1 Pathway in Embryos at Stages 13–14

	Transgenic Animals [# abnormal hemisegments/total # hemisegments (%)]		
Line	Heterozygous	Homozygous[a]	Transheterozygous
KA16B[b]	17/72 (24%)	147/182 (81%)	
KA26A	15/218 (7%)	176/332 (53%)	
KA61A	31/190 (16%)	78/128 (61%)	
KA16c	ND[c]	110/212 (52%)	
KC137A	29/155 (19%)	105/194 (54%)	
KC163A	ND	21/179 (12%)	
KC168A	5/32 (16%)	81/158 (51%)	
K14A	ND	2/180 (1%)	
K21g	ND	1/128 (0.8%)	
K103a	ND	1/148 (0.7%)	
KβG	ND	0/274 (0%)	
KA16B × KC137A			136/216 (63%)
KA16B × KC168A			146/184 (79%)
Wild type[d]		1/292 (0.3%)	

[a] Homozygous embryos were identified by the absence of β-gal staining as driven by a *lacZ* transgene on the balancer chromosome (except wild type; see below).

[b] Line KA16B has two copies of the KA P element inserted on the second chromosome. Thus, embryos have either two or four copies in heterozygous and homozygous embryos, respectively.

[c] ND, not determined.

[d] Wild-type, homozygous embryos (not transgenic) are w^{1118}, the parental strain from which all other transgenic strains were derived.

with the patches of KA staining observed with MAb 10F4 along the MP1 and FN3 pathways at later stages (data not shown).

MAb 10F4 should also recognize the CaM-binding peptide expressed in the A transformant lines. However, we were unable to observe the expression of this peptide with histological methods. This may be due to poor or diffuse expression, fast turnover of the peptide in vivo, or technical difficulties in detecting such a small basic peptide. The CaM-binding peptide is arginine- and lysine-rich (see Experimental Procedures for sequence) and could be readily targeted for degradation; in addition, the predicted diffuse intracellular distribution would increase the difficulty of immunocytochemical observation of this peptide.

The vMP2 and MP1 Pathway Growth Cones Show Specific Defects in Extension and Guidance When Ca^{2+}-CaM Signaling Is Disrupted

We used MAbs 22C10 and 1D4 to examine the development of the vMP2 and MP1 pathways during stages 13–14. Embryos from the 1 KβG, 7 K, and 9 A transformant lines were indistinguishable from wild-type embryos (Figure 5A; our wild-type embryos were w^{1118}, the parental strain from which all of the transgenic strains were derived). However, the embryos from all 11 KA and 8 KC transformant lines exhibited defects in the formation of these first two longitudinal axon pathways. We analyzed the pathfinding errors in greater detail in 3 KA and 3 KC lines. These lines were all homozygous viable, and thus the phenotypic effects resulting from any potential gene disruption at the site of the transposon insertion are expected to be minimal. No abnormal changes in neural cell fate or increases in cell death were observed in KA embryos stained with antibodies against the segmentation genes *engrailed* and *even skipped*. The 6 different transformant lines exhibited the same spectrum of pathfinding errors, although the severity of the phenotypes was more pronounced in KA lines. The following description applies to both KA (Figures 5B and 5C) and KC (Figure 5D) lines.

Embryos homozygous for the KA or KC inserts display two classes of mutant phenotypes at stages 13–14: stalls in axon extension and errors in axon guidance. The initial outgrowth and orientation of the dMP2 and vMP2 growth cones at stage 12 appear relatively normal as assayed with MAb 22C10; this is a stage at which these growth cones are already expressing KA, and we presume KC as well. However, by mid stage 13, the first phenotype (the stall in growth cone extension) becomes quite pronounced for dMP2 and vMP2 in many segments (Figures 5B and 5D; summarized in Figure 1B).

This stalled extension phenotype is often transient. Many segments at stage early 14 exhibit stalls in dMP2 and/or vMP2 extension. In some cases, stalls (i.e., gaps in the vMP2 and MP1 pathways) are still evident at stage 16, the oldest embryos we have examined. During stages 13–14, the dMP2 growth cone typically stalls in one of two locations. In many segments, dMP2 remains in extensive contact with the aCC cell body or initial axon segment and does not turn and extend posteriorly (Figures 5B and 5D; summarized in Figure 1B, #1); it fails to defasciculate from aCC, a contact that in wild type is quite transient. In other segments, dMP2 remains adjacent to SP1 and LGX (Figures 5B and 5D; summarized in Figure 1B, #2). Similarly, the vMP2's growth cone (and pCC as assayed with MAb 1D4) stalls in the region of its specialized contact with SP1 (or perhaps the unstained LGX glial cell just lateral to SP1; summarized in Figure 1B). The rate of extension of aCC into the periphery is also sometimes stalled in KA and KC lines compared with wild-type embryos.

The second major phenotype, errors in axon guidance (summarized in Figure 1C), is first seen at stage late 13 and becomes quite pronounced by stage early 14. In KA

and KC homozygous embryos, at the location in the middle of LGX where dMP2 normally defasciculates from pCC to pioneer the separate MP1 pathway (Figure 1A), instead we often observe that dMP2 fails to defasciculate from pCC and continues to extend along the vMP2 pathway, and thus only one axon pathway forms (Figure 5C; summarized in Figure 1C). Thus, the dMP2 and MP1 growth cones turn more medially than would normally occur in wild type and extend closer to the midline as they follow the vMP2 pathway.

At stages 13–14, the MP1 pathway appeared normal in the 1 KβG and 7 K lines, whereas abnormalities were seen in every homozygous embryo from all 11 KA and 8 KC lines. We quantified the penetrance of the MP1 pathway phenotype at stages 13–14 by counting the number of hemisegments in which the MP1 pathway between the segments had not formed in embryos from 4 KA, 3 KC, 1 KβG, and 3 K transformant lines (Table 1). The penetrance of the MP1 pathway mutant phenotype in the 4 KA and 3 KC lines ranged from 12% to 81% of hemisegments for homozygotes and 7%–24% for heterozygotes. Homozygous embryos of any 1 KA or KC line have at least a 3-fold higher penetrance of phenotype than the respective heterozygous embryos. KA line 16B as homozygotes showed the most penetrant phenotype (81%). This line contains two independent P-element inserts on the same chromosome, and thus the homozygotes contain four copies of the KA gene.

The KA and KC fusion proteins appear to be able to act cooperatively in increasing the penetrance of these phenotypes, further suggesting that they are both interfering with the same signaling process. Transheterozygote embryos carrying two copies of KA (i.e., line KA16B) and one copy of KC (KC137A or KC168A) show a higher percentage of abnormal hemisegments than the sum of both lines alone. We observed MP1 pathway abnormalities in 63%–79% of hemisegments in these transheterozygous embryos as compared with 24% for KA16B, 19% for KC137A, and 16% for KC168A heterozygous embryos (Table 1).

The MP1 Pathway Axons Abnormally Cross the Midline When Ca^{2+}-CaM Signaling Is Disrupted in Their Growth Cones

After stage early 14, it becomes increasingly difficult with the available probes (MAbs 22C10 and 1D4) to distinguish individual growth cones. However, from this time on, we can observe the trajectories of specific axon pathways and the behavior of axons that normally fasciculate tightly in these pathways using MAb 1D4 to stain the axons in the vMP2, MP1, and FN3 pathways (Lin et al., 1994). The most striking KA and KC mutant phenotype is that in many segments the MP1 pathway freely crosses the midline (Figures 6B–6D; summarized in Figure 7B). The crossovers tend to take place in the region around the posterior commissure or between the two commissures. In some segments, there is only a single MP1 pathway on one side of the segment (Figure 6B; the contralateral MP1 pathway having crossed over in a neighboring segment), whereas in other segments, disrupted MP1 pathways are observed on both sides of the midline (Figures 6C and 6D). Moreover, we occasionally see FN3 pathway axons cross the midline as well (Figure 6B). In some respects, this mutant phenotype at stage 16 is reminiscent of the MP1 pathway midline crossovers observed in embryos mutant for the *roundabout* (*robo*) gene (Seeger et al., 1993).

In wild-type embryos, the MP1 pathway never crosses the midline. Clearly, in KA and KC homozygous mutant embryos, the axons in the MP1 pathway no longer respect this midline boundary and instead freely cross the midline. We do not know which MP1 pathway growth cone(s) is the first to cross the midline. The dMP2 and MP1 growth cones are good candidates. They remain abnormally fasciculated with the vMP2 pathway at stage 13 and by stage early 14 extend much closer to the midline than would normally occur. It is possible that in some segments these growth cones might cross the midline around the posterior commissure, where they are only a short distance from their contralateral homologs. Alternatively, it could be that subsequent follower growth cones that also express KA are the first to cross the midline at this location. Regardless of which axons are the first to cross, it appears that all of the MP1 pathway axons are capable of crossing the midline and do so repeatedly in multiple segments in KA and KC lines.

The final phenotype observed in these KA and KC stage 16 mutant embryos is that axons do not remain as tightly fasciculated in the specific MP1 and FN3 pathways. Rather, axons are observed to wander in and out of any given pathway; in some cases, whole bundles of axons shift from one pathway to another (Figure 6B). Both of these phenotypes correlate with the observation that the ftz_{ng} element drives expression in most if not all of the axons in the MP1 and FN3 pathways (Lin et al., 1994).

Discussion

Growth cones can detect and discriminate between a wide variety of different types of guidance cues. How many of these guidance cues are transduced through Ca^{2+}-dependent signaling mechanisms is unknown. To study directly the role of CaM signaling in transducing growth cone guidance cues in vivo, we designed a system that selectively disrupts Ca^{2+}–CaM function in specific growth cones in the developing organism. To this end, we combined the power of genetics in Drosophila with the ability to use specific antibody probes to follow the growth cones that normally pioneer the first two longitudinal axon pathways, the vMP2 and MP1 pathways, and the subsequent trajectories of these axon pathways. Much is already known about the behavior of these growth cones and the development of these pathways (e.g., Lin et al., 1994; Fetter et al., unpublished data), and thus we should be able to detect even subtle defects in growth cone behavior. By specifically disrupting Ca^{2+}–CaM signaling in these growth cones in vivo, we have shown that Ca^{2+}–CaM signaling plays an important role in the events of growth cone extension and guidance.

We created minigenes that encode novel proteins designed to inhibit Ca^{2+} or CaM signaling in the growth cone

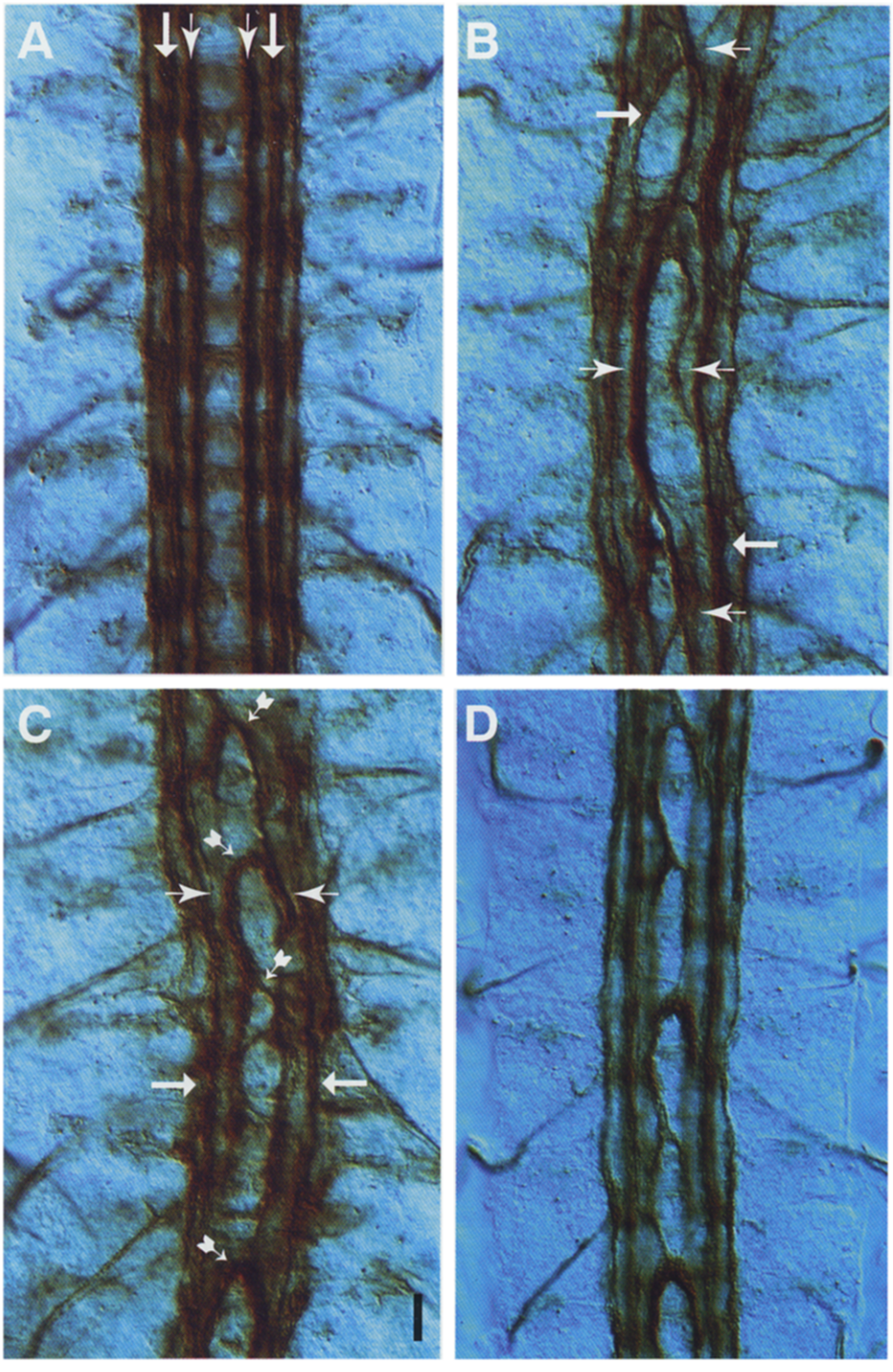

Figure 6. The MP1 Pathway Abnormally Crosses the Midline in KA and KC Mutant Embryos

Photographs of stage 16 wild-type (A), KA (B and C), and KC (D) embryos stained with MAb 1D4 (anti-fasciclin II).

(A) In wild-type embryos, MAb 1D4 reveals the axons in three distinct longitudinal pathways, including the MP1 pathway (white arrow with thin shaft), the FN3 pathway (white arrow with thick shaft), and another more lateral pathway.

(B–D) The most striking KA and KC mutant phenotype is that in many segments the MP1 pathway freely crosses the midline (feathered white arrow in [C]). The crossovers tend to take place in the region around the posterior commissure, or between the two commissures. In some segments, there is only a single MP1 pathway on one side of the segment (B), whereas in other segments, disrupted MP1 pathways are observed on both sides of the midline (C and D). We occasionally see FN3 pathway axons cross the midline (B). Bar, 10 μm.

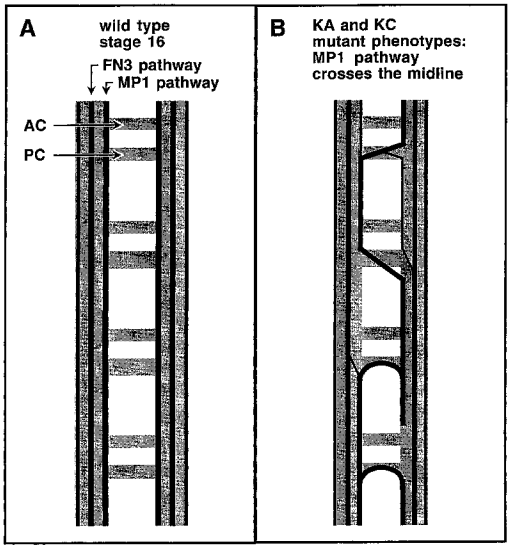

Figure 7. Summary of MP1 Pathway Phenotypes in KA and KC Stage 16 Mutant Embryos

Summary diagram showing the pattern of MAb 1D4 (anti-fasciclin II) staining of three prominent longitudinal axon pathways in wild-type (A) versus KA and KC (B) stage 16 embryos. The most striking and consistent phenotype observed in KA and KC mutant embryos at this stage is the MP1 pathway abnormally crossing the midline in multiple segments. See text for further discussion. AC, anterior commissure; PC, posterior commissure.

and used a specific enhancer element (the ftz_{ng} element; Hiromi et al., 1985) to express these fusion proteins in the neurons whose axons pioneer the vMP2 and MP1 pathways. We used the motor domain of kinesin (Giniger et al., 1993) to target these fusion proteins for the growth cone. The fusion proteins were designed to block CaM function by targeting to the growth cone either a CaM antagonist peptide (the KA construct) or a Ca^{2+}-binding protein in the form of a kinesin fusion protein version of CaM (the KC construct).

Both the KA and KC minigenes led to dramatic mutant phenotypes that were strikingly similar in their defects, dose-dependent in their penetrance, and cooperative in their action. At stages 13–14, when we could monitor the behavior of four individual identified growth cones (pCC, vMP2, dMP2, and MP1) that all express KA and presumably KC as well, we observed two major mutant phenotypes: stalls in axon extension (often at specific choice points) and errors in axon guidance (also often at specific choice points). At stage 16, when we could observe the trajectory of two major longitudinal axon pathways (the MP1 and FN3 pathways) and the axons that normally fasciculate in them, we observed two major phenotypes: the MP1 pathway no longer respects the midline boundary and instead freely crosses the midline, and axons that would normally fasciculate faithfully in one particular pathway instead wander from one pathway to another. All of these phenotypes were observed in multiple independent KA and KC lines. In contrast, we observed the normal behavior of the vMP2 and MP1 growth cones at stages 13–14, and the normal trajectory of the MP1 pathway at stage 16 in control embryos expressing either the kinesin motor domain alone (K), the kinesin–β-gal construct (KβG), or the antagonist peptide alone (A). Thus, it appears on the one hand that it is not the kinesin domain alone that causes the mutant phenotypes, and yet on the other hand, the kinesin domain is necessary to target these Ca^{2+}–CaM inhibitors to the growth cone in order to observe these phenotypes.

The in vivo defects in growth cone behavior and axon pathway trajectory observed in the KA and KC mutants suggest that Ca^{2+}–CaM signaling in the growth cone is required both for regulating axon extension, particularly at certain choice points, and for transducing critical guidance information, including whether to defasciculate at specific choice points and whether to cross the midline. It is striking that both the KA and KC transformants display similar phenotypes, and that transheterozygous embryos containing copies of both KA and KC inserts show enhanced penetrance of these phenotypes. KA can only inhibit CaM function, whereas KC could in principle function in several different fashions, including either the inhibition or enhancement of CaM function. For the latter to occur, KC would have to function by providing additional functional CaM in the growth cone. Arguing against this possibility are the observations that KC lines show the same mutant phenotypes as do KA lines, that these phenotypes are displayed with equal penetrance, and most importantly, that KC and KA cooperatively enhance each other in transheterozygous mutant embryos. Were KC to enhance rather than inhibit CaM function, it would be expected to suppress rather than enhance the KA mutant phenotype.

Our data are more consistent with models in which KC functions as a dominant inhibitor of CaM function. The similarity in phenotype and penetrance of KC and KA suggests that the major route for Ca^{2+} signaling in the growth cone operates via CaM function. The dominant inhibitory function of KC could occur in either of two ways: by binding Ca^{2+} and thus inhibiting the activation of CaM, or by binding to CaM target proteins but failing to activate them. The first model for KC action is consistent with the body of CaM structure–function evidence (e.g., Beckingham, 1991) and the ability of KC to bind phenyl-Sepharose in a Ca^{2+}-dependent manner. Studies on CaM activation of target proteins (e.g., MLCK or CaMKII) predict that the globular Kinesin domain (~600 amino acids) should sterically hinder KC activation of CaM-dependent enzymes. However, the second model for KC action as a dominant inhibitor is also possible. Mutagenesis of CaM indicates that CaM has different structural requirements for binding to versus activation of various target proteins (Zot et al., 1990; VanBerkum and Means, 1991; Persechini et al., 1994). In either case, KC appears to block Ca^{2+}–CaM function in the growth cone in a fashion very similar to KA. It is satisfying that these two proteins (KA and KC) provide two different ways of interfering with Ca^{2+}–CaM function and both give rise to identical mutant phenotypes. These results suggest that, in the growth cone, CaM is a major downstream effector of Ca^{2+} signaling, although other CaM-independent pathways cannot be ruled out.

Disrupting Ca^{2+} signaling in the pCC, vMP2, dMP2, and

MP1 growth cones leads to stalls in axon extension and errors in axon guidance, including the failure to defasciculate at a specific choice point. Are the stalls in extension related to the errors in guidance, or are they two independent functions? When specific growth cones are stalled, the stalls tend to occur at locations where these growth cones normally display a transient affinity for some particular cell surface, and then detach as they turn and extend in another direction. For example, the dMP2 growth cone stalls where it contacts the aCC axon (Figure 1B, #1) or where it contacts the LGX glial cell (Figure 1B, #2). Similarly, pCC and vMP2 stall where they contact the SP1 neuron or LGX glial cell.

These stalls in axon extension could be due to a defect in the motility apparatus. Alternatively, the stalls could result from a failure to respond properly to the next sequential guidance cue and/or their inability to detach or defasciculate from what should have been a transient contact. Arguments can be put forward for both explanations. For example, overexpression of CaMKII (a major target enzyme for CaM) in neuroblasts results in increased neurite outgrowth (Goshima et al., 1993). Thus, a reduction in CaM function in KA and KC transformants might inhibit axon extension. Alternatively, Ca^{2+} signaling might be required to detach a growth cone from one guidance substrate, thereby allowing it to respond to new guidance cues. CaM regulation of calcineurin, a CaM-dependent phosphatase, has been implicated in the regulation of neutrophil migration. In these neutrophils, injection of calcineurin inhibitor peptides appears to prevent the release of cells from attachment sites by inhibiting the dephosphorylation of integrin (Hendey et al., 1992). Perhaps neural cell adhesion molecules can also be reversibly regulated by Ca^{2+}–CaM-dependent mechanisms.

The growth cone stalls we observe in KA and KC embryos are not necessarily related directly to deficits in the motility apparatus. The initial events of neurite outgrowth occur normally in these mutants (even though KA is expressed at this stage), and the locations of the stalls are relatively consistent and tend to occur at major choice points, where axon pathways intersect or where growth cones make major changes in their trajectory. The specificity of the locations of these stalls suggests that the decreases in Ca^{2+} signaling in KA and KC mutants may hamper the ability of the growth cone to transduce new guidance cues or to change from one substrate to another. Extensive in vitro analysis has shown that neural cell adhesion molecule–mediated neurite outgrowth requires Ca^{2+} signaling (e.g., Doherty and Walsh, 1994). Perhaps in KA and KC mutants, cell adhesion molecule–mediated guidance cues (or other types of guidance cues) can no longer be transduced properly into functional signals for growth cone motility.

The most striking of the KA and KC mutant phenotypes is that observed at stage 16 in the remarkable ability of the MP1 pathway to move back and forth across the midline freely. In wild-type embryos, the MP1 pathway never crosses the midline. These results suggest that normal Ca^{2+}–CaM function is required in the growth cones of the MP1 pathway neurons in order for them to remain on their own side and to respect the putative repulsive signal at the midline (Seeger et al., 1993; Tear et al., 1993).

In the developing CNS of the Drosophila embryo, the decision of whether growth cones cross the midline is tightly regulated. About 10% of the CNS interneurons project their axons only on their own side, in some cases extending quite close to the midline and through commissural regions without crossing the midline (Tear et al., 1993). The other 90% of these CNS interneurons initially project their axons across the midline in one of the two major commissures and then turn either anteriorly or posteriorly in a particular longitudinal axon tract on the other side. The behavior of these growth cones after crossing the midline is markedly different from their behavior before reaching it: they typically show no affinity for the homologous longitudinal pathway on their own side, but once they cross the midline, they change their behavior as they turn and follow the same pathway on the other side. Moreover, having crossed the midline, these growth cones rarely cross again, suggesting that they have either down-regulated their responsiveness to the putative midline attractant or up-regulated their responsiveness to the putative repellent.

Genetic analysis in Drosophila has revealed a few perturbations that lead MP1 pathway growth cones to cross the midline abnormally, and several other genetic manipulations that alter the behavior of these same growth cones without causing them to cross the midline. For example, genetic manipulations that lead to the loss or failure to differentiate of certain midline cells can result in MP1 pathway axons incorrectly crossing the midline (Klämbt et al., 1991; Menne and Klämbt, 1994), but these midline cells are clearly present and differentiate normally in KA and KC mutants; moreover, the ftz_{ng} element does not drive expression in these cells.

The midline crossing of axons is not simply a secondary consequence of the failure of dMP2 to defasciculate from the vMP2 pathway. In separate studies, when the level of fasciclin II was increased selectively on these same growth cones and axons, dMP2 often failed to defasciculate from the vMP2 pathway at stage 13, and yet at stage 16, these abnormal pathways nevertheless clearly remained on their own side and did not cross the midline (Lin et al., 1994). In another set of experiments, the same ftz_{ng} element was used to ablate these same neurons selectively using diphtheria toxin (D. Lin, V. Auld, and C. S. G., unpublished data). Large gaps and stalls in the formation of the MP1 pathway were observed at stage 13, and yet at stage 16, the remaining MP1 pathway axons did not cross the midline. Thus, not every perturbation in these axons causes them to cross the midline. On the contrary, very few genetic manipulations cause these axons to cross the midline.

The midline crossings of MP1 pathway axons in KA and KC mutant embryos are reminiscent of the midline crossings observed at stage 16 in *robo* mutant embryos (Seeger et al., 1993). In *robo*, the pCC, vMP2, dMP2, and MP1 growth cones cross the midline as soon as their growth cones reach the anterior commissure. The axons of many subsequent follower growth cones then also cross the mid-

line, and by stage 16, the MP1 pathway crosses the midline in many locations and appears quite similar to what we describe here in KA and KC mutant embryos (Figure 6; summarized in Figure 7).

If indeed, as has been proposed previously, there are midline repulsive signals that prevent certain growth cones from crossing the midline (reviewed by Tear et al., 1993; Goodman, 1994), then there are apparently two totally independent genetic methods of overcoming this midline repulsion and allowing the MP1 pathway axons to cross the midline, the first involving the loss-of-function in the *robo* gene and the second involving the inhibition of Ca^{2+}–CaM signaling in the growth cone. Previous studies on growth cone collapse factors in vitro have suggested that certain factors may mediate growth cone collapse via a Ca^{2+} signaling mechanism (Bandtlow et al., 1993), whereas others may not (Ivins et al., 1991). The results described in the present paper suggest that, in the developing CNS of Drosophila, at least one type of putative midline repulsive signal that prevents MP1 pathway growth cones from crossing the midline may require normal Ca^{2+}–CaM signaling for its proper function.

Experimental Procedures

Construction of kinesin Fusion Proteins and Germ-Line Transformation

The linker region between the kinesin and the β-gal portions of the pKZtrap plasmid (Giniger et al, 1993) contained EcoRI, SmaI, and BamHI restriction endonuclease sites as shown: GAT GCC AGA ATT CCC GGG GAT CCC (reading frame denoted in triplets). A 2 kb NotI–BamHI fragment was removed and ligated into pBluescript KS(+) to create pBS-kin encoding the kinesin motor domain (K). In this way, 35 additional amino acids (from the CCC of the SmaI site: GDPPAAGLRYQAYRYRRPRGGARYAANSALVPISS) were added to the C-terminus of kinesin before a stop codon was read. For KA, the CaM regulatory domain of chicken MLCK was removed as a 0.170 kb BamHI–SstI fragment from the bacterial expression vector pMK40K-Bam (Bagchi et al., 1992), blunt ended (mung bean nuclease), and ligated into the SmaI site of pBS-kin. A total of 44 amino acids were added to the C-terminus of kinesin: QKDTKNMEAKKLSKDRMKKYMARRKWQKTGHAVRAIGRLSSQSQ (the CaM-binding domain is underlined). The KC transformant was created by removing the CaM coding sequence (148 amino acids) from pCaMPL as a 0.765 kb NcoI–XbaI fragment (VanBerkum and Means, 1991). The blunt-ended fragment (mung bean nuclease) was ligated into the SmaI site of pBS-kin. Clones were sequenced to confirm the reading frame and the sequence of the antagonist peptide, CaM, or the amino acid extension on K. The entire fusion protein was removed as a NotI–Asp-718 fragment, blunt ended (Klenow), and ligated into a blunt-ended (Klenow) NotI site of p2A/N-ftz-tx. This latter plasmid was created by blunt-end ligation of an approximately 1.5 kb XbaI–XmnI fragment encoding the ftz_{ng} element into the 5′ XbaI site of the transformation vector pCASP 2A/N (provided by D. Lin).

The construct encoding the CaM antagonist peptide alone (A) was created by removing the 0.17 kb BamHI–SstI fragment of pMK40K and inserting it into pBluescript KS(+). A SstI–SmaI fragment was then removed, blunt ended (T4 polymerase), and ligated into a blunt-ended XbaI site (Klenow) of pftzATG(1X). (pftzATG(1X) is a modified version of $pftz_{NG}$ATG [provided by D. Van Vactor] such that the XbaI site at the 5′ end of the ftz_{ng} element was removed by a partial XbaI digest, blunt ended, and religated.) In this way, the first 9 amino acids (MPAIVLGGI) of HSP70 were added to the N-terminus of the CaM regulatory domain as found in pMK40K (or KA). The A minigene was removed from this kanamycin vector as an EcoRI fragment and inserted into the EcoRI sites of p2A/Nftz(tx).

The p2A/N-kinesin fusion plasmids were mixed in a 3:1 ratio with the helper plasmid pUChsπΔ2-3 (40 μg/ml final concentration) and used to transform w^{1118} embryos (Rubin and Spradling, 1982). Transformed flies were maintained in standard culture media as balanced stocks over CyO or TM3 balancers carrying a transposon encoding the *lacZ* gene under the regulation of the neural-specific *elav* promoter (*elav–β-gal*).

Immunocytochemistry

Immunocytochemistry was performed using the previously described method (Klämbt et al., 1991), except we used 3.7% formaldehyde as the fixative. The MAbs 22C10, 1D4 (anti-fasciclin II; G. Helt, unpublished data), 3C10 (anti–even skipped), and 4D9 (anti-engrailed) were used at 1:5 dilutions. Horseradish peroxidase (HRP)-conjugated goat anti-mouse secondary antibody was used at a 1:400 dilution. Embryos carrying the *elav–β-gal* transgene balancer chromosome(s) were identified by X-gal activity staining for 2 hr at 37°C (Klämbt et al.,1991). KA expression in embryos was determined using a rat MAb 10F4 (see below) diluted 1:1 and detected using the Vectastain ABC kit (Vector Laboratories).

Antibody Production

A synthetic peptide analog of the CaM regulatory domain, (C)EAKKLSKDRMKKYMARRKWQKTGHAVRAIGRLSS, was synthesized by fluorinylmethoxycarbonyl (FMOC) chemistry in an ABI 431A synthesizer. The peptide was purified by reverse-phase high pressure liquid chromatography and characterized by mass spectrometry (Hewlett-Packard 5989A). The peptide was conjugated to keyhole limpet hemocyanin using Sulfo-MBS (Pierce). Rats were injected, and once an immune response was detected, rat MAb 10F4 was isolated using standard techniques.

Microtubule Co-Sedimentation

Embryos were harvested and dechorinated as previously described (Saxton et al., 1988). After washing, embryos were transferred to test tubes on ice and rinsed twice with ice-cold PEM buffer (0.1 M Pipes [pH 7.0], 5 mM EDTA, 2 mM $MgSO_4$, 1 mM phenylmethylsulfonyl fluoride). Embryos were homogenized in 0.5–1.0 ml of PEM buffer plus additional protease inhibiors (Saxton et al., 1988) for 60 s using a Brinkmann polytron. Homogenates were centrifuged at 20,000 × g for 20 min (4°C), and the supernatants were again spun for 1 hr at 50,000 rpm in a TLA100.3 rotor (4°C). Microtubule polymerization was induced in the clarified supernatant by adding taxol (Sigma) and GTP to final concentrations of 20 μM and 1 mM, respectively (Saxton et al., 1988; Vale et al., 1985). After gentle agitation (40 min at room temperature), AMP-PNP was added to 2.5 mM, and the samples were agitated for a further 30 min. Microtubules and associated proteins were sedimented at 50,000 rpm for 30 min (24°C), the pellets enriched for microtubules, kinesin, and the kinesin fusion proteins were resuspended in PEM, and SDS–sample buffer was immediately added.

Western Blot Analysis

Proteins in the microtubule-enriched pellets were separated by electrophoresis on 8% SDS–polyacrylamide gels (O'Farrell, 1975) and transferred to nitrocellulose by standard blotting techniques. Blots were probed with a 1:500 dilution of MAb DK410–2.1 (anti-Kinesin; provided by M. Sheetz), a 1:400 dilution of a mouse anti-β-gal, or a 1:10,000 dilution of the rat serum antibody against the CaM-binding peptide. The HRP-conjugated goat anti-mouse or rat secondary was used (1:15000), and the blot was developed by chemiluminescence (ECL; Amersham). To decrease background staining and remain in antibody excess, the blot was cut at the 100 kDa position, and each portion of the blot was probed and developed separately.

CaM Overlay

Bacterially expressed chicken CaM was purified as described elsewhere (VanBerkum and Means, 1991) and dialyzed overnight in 0.1 M phosphate buffer (pH 7.4). Succinimidyl D-biotin (1 mM; Molecular Probes) was crosslinked to CaM (1.2 mg/ml) for 2 hr at 4°C, and the reaction was terminated by extensive dialysis (C. Rasmussen, personal communication). Replica Western blots were probed with 0.25 μM biotinylated CaM in Tris-buffered saline, plus 10 mg/ml bovine serum albumin and either 4 mM $CaCl_2$ or 8 mM EDTA for 2 hr at room temperature. Bound CaM was detected by using HRP-conjugated streptavidin and developing the blots with diaminobenzidine.

Acknowledgments

We thank Ed Giniger for the kinesin–β-gal construct, David Van Vactor for the *ftz_{ng}–kinesin–β-gal* transformant line, Tony Means and I. C. Bagchi for the CaM and MLCK clones, respectively, Kate Beckingham for the unpublished *calmodulin* mutant *cam1* and *CB21* fly strains, Michael Sheetz for the anti-kinesin MAb, and David King for the synthesized peptide. Zac Candy gave advice and tubulin reagents, and W. M. Saxton, J. Scholey, and Larry Goldstein provided antibodies and other reagents used in initial experiments. Special thanks to Luis Garcia Alonso as M. V. B.'s fly genetics teacher. M. V. B. was a postdoctoral fellow of the Medical Research Council of Canada. C. S. G. is an Investigator of the Howard Hughes Medical Institute.

References

Bagchi, I. C., Huang, Q. H., and Means, A. R. (1992). Identification of amino acid essential for calmodulin binding and activation of smooth muscle myosin light chain kinase. J. Biol. Chem. *267*, 3024–3029.

Bandtlow, C. E., Schmidt, M. F., Hassinger, T. D., Schwab, M. E., and Kater, S. B. (1993). Role of intracellular calcium in NI-35-evoked collapse of neuronal growth cones. Science *259*, 80–83.

Beckingham, K. (1991). Use of site-directed mutations in the individual Ca^{2+}-binding sites of calmodulin to examine Ca^{2+}-induced conformation changes. J. Biol. Chem. *266*, 6027–6030.

Bentley, D., Guthrie, P. B., and Kater, S. B. (1991). Calcium ion distribution in nascent pioneer axons and coupled preaxonogenesis neurons in situ. J. Neurosci. *11*, 1300–1308.

Bowman, B. R., Peterson, J. A., and Stull, J. T. (1992). Pre-steady state kinetics of the activation of rabbit skeletal muscle myosin light chain kinase by Ca^{2+}/calmodulin. J. Biol. Chem. *267*, 5346–5354.

Callahan, C. A., and Thomas, J. B. (1994). Tau-β-galactosidase, an axon-targeted fusion protein. Proc. Natl. Acad. Sci. USA *91*, 5972–5976.

Chattopadhyaya, R., Meador, W. E., Means, A. R., and Quiocho, F. A. (1992). Calmodulin structure refined at 1.7 Å resolution. J. Mol. Biol. *228*, 1177–1192.

Cypher, C., and Letourneau, P. C. (1992). Growth cone motility. Curr. Opin. Cell Biol. *4*, 4–7.

Davenport, R. W., and Kater, S. B. (1992). Local increases in intracellular calcium elicit local filopodial responses in Helisoma neuronal growth cones. Neuron *9*, 405–416.

Doe, C. Q., Hiromi, Y., Gehring, W. J., and Goodman, C. S. (1988). Expression and function of the segmentation gene *fushi tarazu* during Drosophila neurogenesis. Science *239*, 170–175.

Doherty, P., and Walsh, F. S. (1994). Signal transduction events underlying neurite outgrowth stimulated by cell adhesion molecules. Curr. Opin. Neurobiol. *4*, 49–55.

Doyle, K. E., Kovalick, G. E., Lee, E., and Beckingham, K. (1990). *Drosophila melanogaster* contains a single calmodulin gene: further structure and expression studies. J. Mol. Biol. *213*, 599–605.

Gao, Z. H., Krebs, J., VanBerkum, M. F., Tang, W. J., Maune, J. F., Means, A. R., Stull, J. T., and Beckingham, K. (1993). Activation of four enzymes by two series of calmodulin mutants with point mutations in individual Ca^{2+} binding sites. J. Biol. Chem. *268*, 20096–20104.

Giniger, E., Wells, W., Jan, L. Y., and Jan, Y. N. (1993). Tracing neurons with a kinesin-β-galactosidase fusion protein. Roux's Arch. Dev. Biol. *202*, 112–122.

Gnegy, M. E. (1993). Calmodulin in neurotransmitter and hormone action. Annu. Rev. Pharmacol. Toxicol. *33*, 45–70.

Goodman, C. S. (1994). The likeness of being: phylogenetically conserved molecular mechanisms of growth cone guidance. Cell *78*, 353–356.

Goodman, C. S., and Shatz, C. J. (1993). Developmental mechanisms that generate precise patterns of neuronal connectivity. Cell *72*/Neuron *10* (Suppl.), 77–98.

Goshima, Y., Ohsako, S., and Yamauchi, T. (1993). Overexpression of Ca^{2+}/calmodulin-dependent protein kinase II in Neuro2a and NG108-15 neuroblastoma cell lines promotes neurite outgrowth and growth cone motility. J. Neurosci. *13*, 559–567.

Gough, A. H., and Taylor, D. L. (1993). Fluorescence anisotropy imaging microscopy maps calmodulin binding during cellular contraction and locomotion. J. Cell Biol. *121*, 1095–1107.

Hanson, P. I., and Schulman, H. (1992). Neuronal Ca^{2+}/calmodulin-dependent protein kinases. Annu. Rev. Biochem. *61*, 559–601.

Hendey, B., Klee, C. B., and Maxfield, F. R. (1992). Inhibition of neutrophil chemokinesis on vitronectin by inhibitors of calcineurin. Science *258*, 296–299.

Hinrichsen, R. D. (1993). Calcium and calmodulin in the control of cellular behavior and motility. Biochem. Biophys. Acta *1155*, 277–293.

Hiromi, Y., Kuroiwa, A., and Gehring, W. J. (1985). Control elements of the Drosophila segmentation gene *fushi tarazu*. Cell *43*, 603–613.

Ikura, M., Clore, G. M., Gronenborn, A. M., Zhu, G., Klee, C. B., and Bax, A. (1992). Solution structure of a calmodulin-target peptide complex by multidimensional NMR. Science *256*, 632–638.

Ivins, J. K., Raper, J. A., and Pittman, R. N. (1991). Intracellular calcium levels do not change during contact-mediated collapse of chick DRG growth cone structure. J. Neurosci. *11*, 1597–1608.

Janmey, P. A. (1994). Phosphoinositides and calcium regulators of cellular actin assembly and disassembly. Annu. Rev. Physiol. *56*, 169–191.

Kater, S. B., and Mills, L. R. (1991). Regulation of growth cone behavior by calcium. J. Neurosci. *11*, 891–899.

Kennedy, T. E., Serafini, T., de la Torre, J. R., and Tessier-Lavigne, M. (1994). Netrins are diffusible chemotropic factors for commissural axons in the embryonic spinal cord. Cell *78*, 425–435.

Klämbt, C., Jacobs, J. R., and Goodman, C. S. (1991). The midline of the Drosophila central nervous system: a model for the genetic analysis of cell fate, cell migration, and growth cone guidance. Cell *64*, 801–815.

Knighton, D. R., Pearson, R. B., Sowadski, J. M., Means, A. R., Ten Eyck, L. F., Taylor, S. S., and Kemp, B. E. (1992). Structural basis of the intersteric regulation of myosin light chain kinases. Science *258*, 130–135.

Kolodkin, A. L., Matthes, D. J., O'Connor, T. P., Patel, N. H., Bentley, D., and Goodman, C. S. (1992). Fasciclin IV: sequence, expression, and function during growth cone guidance in the grasshopper embryo. Neuron *9*, 831–845.

Kolodkin, A. L., Matthes, D. J., and Goodman, C. S. (1993). The *semaphorin* genes encode a family of transmembrane and secreted growth cone guidance molecules. Cell *75*, 1389–1399.

Kovalick, G. E., and Beckingham, K. (1992). Calmodulin transcription is limited to the nervous system during Drosophila embryogenesis. Dev. Biol. *150*, 33–46.

Lee, G. (1993). Non-motor microtubule-associated proteins. Curr. Opin. Cell Biol. *5*, 88–94.

Lin, D. M., Fetter, R. D., Kopczynski, C., Grenningloh, G., and Goodman, C. S. (1994). Genetic analysis of Fasciclin II in Drosophila: defasciculation, refasciculation, and altered fasciculation. Neuron *13*, 1055–1069.

Luo, Y., Raible, D., and Raper, J. A. (1993). Collapsin: a protein in brain that induces the collapse and paralysis of neuronal growth cones. Cell *75*, 217–227.

McCarron, J. G., McGeown, J. G., Reardon, S., Ikebe, M., Fay, F. S., and Walsh, J. V., Jr. (1992). Calcium-dependent enhancement of calcium current in smooth muscle by calmodulin-dependent protein kinase II. Nature *357*, 74–77.

Meador, W. E., Means, A. R., and Quiocho, F. A. (1992). Target enzyme recognition by calmodulin: 2.4 Å structure of a calmodulin-peptide complex. Science *257*, 1251–1255.

Meador, W. E., Means, A. R., and Quiocho, F. A. (1993). Modulation of calmodulin plasticity in molecular recognition on the basis of X-ray structures. Science *262*, 1718–1721.

Means, A. R., Bagchi, I. C., VanBerkum, M. F., and Kemp, B. E. (1991). Regulation of smooth muscle myosin light chain kinase by calmodulin. Adv. Exp. Med. Biol. *304*, 11–24.

Menne, T. V., and Klämbt, C. (1994). The formation of commissures

in the Drosophila CNS depends on the midline cells and on the Notch locus. Development *120*, 123–133.

O'Farrell, P. H. (1975). High resolution two-dimensional electrophoresis of proteins. J. Biol. Chem. *250*, 4007–4021.

Persechini, A., McMillan, K., and Leakey, P. (1994). Activation of myosin light chain kinase and nitric oxide synthetase activities by calmodulin fragments. J. Biol. Chem. *269*, 16148–16154.

Polak, K. A., Edelman, A. M., Wasley, J. W. F., and Cohan, C. S. (1991). A novel calmodulin antagonist, CGS 9343B, modulates calcium-dependent changes in neurite outgrowth and growth cone movements. J. Neurosci. *11*, 534–542.

Rehder, V., and Kater, S. B. (1992). Regulation of neuronal growth cone filopodia by intracellular calcium. J. Neurosci. *12*, 3175–3186.

Rubin, G. M., and Spradling, A. C. (1982). Genetic transformation of Drosophila with transposable element vectors. Science *218*, 348–353.

Saxton, W. M., Porter, M. E., Cohn, S. A., Scholey, J. M., Raff, E. C., and McIntosh, J. R. (1988). Drosophila kinesin: characterization of microtubule motility and ATPase. Proc. Natl. Acad. Sci. USA *85*, 1109–1113.

Schuch, U., Lohse, M. J., and Schachner, M. (1989). Neural cell adhesion molecules influence second messenger systems. Neuron *3*, 13–20.

Seeger, M., Tear, G., Ferres-Marco, D., and Goodman, C. S. (1993). Mutations affecting growth cone guidance in Drosophila: genes necessary for guidance toward or away from the midline. Neuron *10*, 409–426.

Serafini, T., Kennedy, T. E., Galko, M. J., Mirzayan, C., Jessell, T. M., and Tessier-Lavigne, M. (1994). The netrins define a family of axon outgrowth-promoting proteins homologous to C. elegans UNC-6. Cell *78*, 409–424.

Silver, R. A., Lamb, A. G., and Bolsover, S. R. (1990). Calcium hotspots caused by L-channel clustering promote morphological changes in neuronal growth cones. Nature *343*, 751–754.

Skoufias, D. A., and Scholey, J. M. (1993). Cytoplasmic microtubule-based motor proteins. Curr. Opin. Cell Biol. *5*, 95–104.

Tear, G., Seeger, M., and Goodman, C. S. (1993). To cross or not to cross: a genetic analysis of guidance at the midline. Perspect. Dev. Neurobiol. *1*, 183–194.

Trewhela, J. (1992). The solution structures of calmodulin and its complexes with synthetic peptides based on target enzyme binding sites. Cell Calcium *13*, 377–390.

Vale, R. D., Schnapp, B. J., Reese, T. S., and Sheetz, M. P. (1985). Organelle, bead, and microtubule translocations promoted by soluble factors from the squid giant axon. Cell *40*, 559–569.

VanBerkum, M. F. A., and Means, A. R. (1991). Three amino acid substitutions in domain I of calmodulin prevent the activation of chicken smooth muscle myosin light chain kinase. J. Biol. Chem. *266*, 21488–21495.

Weinstein, H., and Mehler, E. L. (1994). Ca^{2+}-binding and structural dynamics in the function of calmodulin. Annu. Rev. Physiol. *56*, 213–236.

Zheng, J. Q., Felder, M., Conner, J. A., and Poo, M.-m. (1994). Turning of nerve growth cones induced by neurotransmitters. Nature *368*, 140–144.

Zot, H. G., Aden, R., Samy, S., and Puett, D. (1990). Fluorescent adducts of wheat calmodulin implicate the amino-terminal region in the activation of skeletal muscle myosin light chain kinase. J. Biol. Chem. *265*, 14796–14801.